Electrodeposition

DOI: 10.1002/anie.201207342

Structural Accelerating Effect of Chloride on Copper Electrodeposition**

*Yuriy I. Yanson and Marcel J. Rost**

Despite the relatively large number of studies of metal electrodeposition, in general, and Cu deposition, in particular, on various length scales by using numerous structural as well as electrochemical techniques,[1] reports of in situ observations of the surface evolution during the actual growth remain scarce. The majority of the deposition studies look at the end result of the growth after the actual deposition process has been completed. By analyzing the deposit, various parameters can be extracted, such as the nucleation energy or kinetic parameters. Sometimes one can even distinguish between one or several mechanisms that are active during the electrodeposition process. However, it is not always possible to precisely determine the deposition mechanisms after the deposition has ended. Moreover, after the termination of the deposition the surface may further evolve as a result of processes such as surface diffusion and dissolution. In addition to the deposition mechanism, the precise influence of additives is also interesting, as they change the deposition process. Additives are inorganic or organic substances that are added to the deposition solution to influence the properties of the final deposit. Additives are widely used not only in electrodeposition, but also in conventional crystallization from supersaturated solutions and even in protein crystallization.[2]

One way to be able to unambiguously identify the active deposition mechanisms and to understand the growth kinetics is to observe the surface of interest during the deposition process.[3] Such experiments have shown to be invaluable for the determination of parameters and mechanisms of electrodeposition and dissolution.[4] In particular, in situ video-rate scanning-tunneling-microscope (STM) studies have demonstrated that dynamic processes during the growth can be observed and characterized on the atomic scale.[5] Besides gaining a deeper understanding of the processes that occur during electrodeposition from simple electroplating solutions, such as the electrolyte containing $CuSO_4$ and H_2SO_4, one can also study the effect of additives on the deposition process. For example, it has been shown that the addition of small amounts of Cl^- into a $CuSO_4$ based plating bath has an accelerating effect on Cu deposition. The exact reason for this accelerating effect of Cl^- is still under debate, although it has been proposed that the formation of complexes of Cl^- and Cu^+ might be responsible for it.[6]

Herein, we present our studies of Cu electrodeposition on the Cu(111) surface from sulfate-containing solutions with and without Cl^- by using our custom-built in situ high-speed electrochemical STM.[7] We find that the specific adsorption of the anions and the formation of the ordered anion adlayers have a profound effect on the morphology of the surface during deposition. In contrast to the chemical acceleration, we propose here, for the first time, a structural scenario that could contribute to the accelerating effect of an additive: in our case the effect of Cl^- ions on Cu electrodeposition. We suggest that the reduction of the critical Cu nucleus size in the presence of Cl^- could lead to a lower nucleation barrier, which leads to faster incorporation of the Cu^{2+} ions into the crystal lattice and thus faster overall deposition kinetics.

We study Cu electrodeposition on large flat (111)-oriented Cu crystallites that were electrodeposited on an Au(111) electrode in the electrochemical cell of our STM. Figure 1a shows an STM image of the surface of such a Cu(111) crystallite during growth in a sulfate-containing electrolyte, which consists of 2 mM $CuSO_4$ and 0.1 M H_2SO_4. We find that the surface of this crystallite shows a high density of screw dislocations. We believe that the growth of Cu mainly takes place at the screw dislocations under our experimental

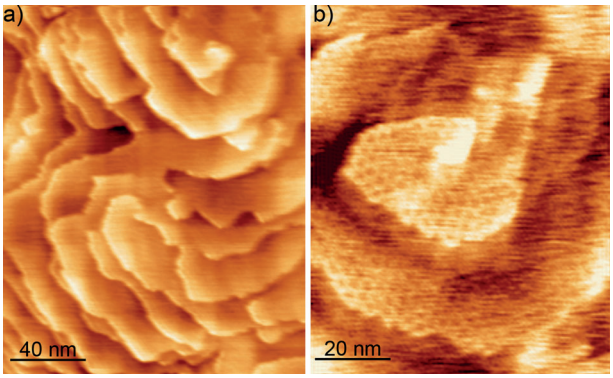

Figure 1. STM images of a Cu crystallite, acquired during Cu electrodeposition from a solution containing 2 mM $CuSO_4$ and 0.1 M H_2SO_4 at a) −86 mV and b) −48 vs. Cu/Cu^{2+}. a) Atomic steps emanate from the screw dislocations that are present everywhere on the surface. We have identified a total of 13 screw dislocations in this image. Image (b) shows a single screw dislocation that exhibits the corrugation of the moiré pattern of the sulfate adlayer on the terraces. Please note that the steps tend to align along the main symmetry axes of the moiré pattern.

[*] Y. I. Yanson, Dr. M. J. Rost
Kamerlingh Onnes Laboratory, Leiden University
Niels Bohrweg 2, 2333CA Leiden (Netherlands)
E-mail: rost@physics.leidenuniv.nl

[**] This research is supported by the Dutch Technology Foundation STW (project number 07720), which is the applied science division of NWO, and the Technology Program of the Ministry of Economic Affairs. We kindly would like to acknowledge J. W. M. Frenken for his comment on the critical nucleus size.

Supporting information for this article is available on the WWW under http://dx.doi.org/10.1002/anie.201207342.

conditions, as we have never observed 2D nucleation of Cu islands on the atomically flat Cu terraces. Figure 1b shows a zoom-in STM image of a single screw dislocation. The periodic corrugation that is visible at the surface, corresponds to the moiré pattern that is formed as a result of the Cu surface reconstruction induced by SO_4^{2-} adsorption.[8,9] The pattern is known to be hexagonal, but stretched along one main symmetry axis. The period of the moiré pattern is 3.45 nm along the stretched direction and 2.70 nm along the other two directions, as determined by Wilms et al.[8] and consistent with our observations.

Figure 2 shows a series of subsequent STM images, where the evolution of a monatomic step during Cu electrodeposition is visible. One can clearly see the major influence of the moiré pattern on the growth morphology of the steps. Firstly, the steps are aligned along the close-packed rows of the moiré

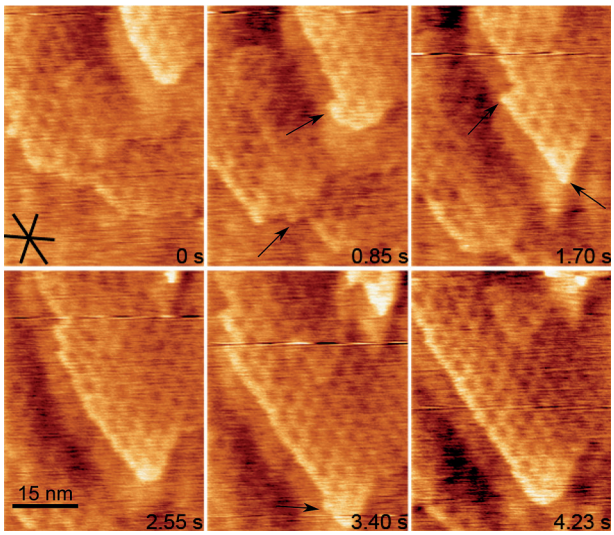

Figure 2. Consecutive STM images of propagating steps at −48 mV vs. Cu/Cu^{2+}. The sulfate-induced moiré pattern is visible on the terraces. The steps are aligned along the main symmetry axes of the moiré pattern, which are depicted by the black lines in the first image. Propagation of the steps proceeds in complete rows of the moiré pattern, although features that are smaller than a moiré unit are observed at the steps (marked by arrows). Also, kinks of the size of a moiré unit are visible. Please note that the halo around the step edges is due to a double tip.

pattern. Secondly, the propagation of the steps proceeds through the formation of entire rows of the moiré structure. Kinks correspond to the end of the rows of complete moiré units. Thus, we can conclude that the moiré units are the stable building blocks during deposition. This finding is consistent with the observation of the formation of Cu adislands that contain an integer number of moiré units during the transition from the disordered sulfate adlayer on Cu(111) to the ordered structure with the moiré pattern.[9] We would like to clarify our definition of the term "building block". We define a building block as the smallest stable unit. One might think that if the growth proceeds in these building blocks, then the whole block (i.e. in this case over 40 atoms) has to assemble at once. However, this is highly improbable. We suggest that the growth of each new moiré unit involves the assembly of a specific cluster of Cu atoms; this cluster can be regarded as the critical nucleus for this process, after which the rest of the moiré unit is completed. If this is so, one expects to observe a modest fraction of incomplete moiré units. This is indeed the case, as is illustrated by the STM images in Figure 2.

To determine the size of the critical nucleus, which is probably smaller than the size of the moiré unit, we can study the distances between steps originating at a screw dislocation. The theory of spiral growth, developed by Burton, Cabrera, and Frank (BCF), predicts that the distance between the spiral coils d is given by:[10]

$$d = 19\, r_{crit} = T_r\, v_{\infty}, \qquad (1)$$

where r_{crit} is the radius of the critical nucleus, T_r is the rotation period of the spiral, and v_∞ is the propagation speed of a straight step (far from the screw dislocation). Although this theory was developed for isotropic growth, Budevski et al. have shown that Equation (1) also holds for polygonized growth spirals regardless of the number of corners.[11] By analyzing four screw dislocations, we obtain $d = 25.8 \pm 4.0$ nm, which leads to a critical nucleus radius of $r_{crit} = 1.4 \pm 0.2$ nm. We obtain a similar value of $r_{crit} = 1.2 \pm 0.4$ nm by using the measured values of $T_r = 5.62 \pm 0.93$ s and $v_\infty = 3.88 \pm 0.70\ nm\,s^{-1}$. This value for the critical radius is very close to the radius of a moiré unit, averaged over the three main directions ($r_m = 1.48$ nm). Hence, one could naively conclude that a moiré unit is not only the smallest stable building block, but it is also the critical nucleus for 2D nucleation. However, we argue that this is not the case, since the BCF model is not fully applicable for our system. Indeed, in the BCF model it is assumed that if the length of a step becomes equal to the diameter of the critical nucleus, the step can propagate freely away from the dislocation. This is obviously not the case in our system, because for a step to propagate, a critical nucleus for the formation of a moiré unit has to be assembled. Additionally, the propagation of a step is not homogeneous, but it is "quantized" in rows of the moiré pattern. We suggest that if the BCF model would be modified to account for such growth, one would find that the distance between steps that emanate from a single screw dislocation is proportional to the size of the stable building block and not to the size of the critical nucleus.

The growth behavior of a monatomic Cu step changes dramatically if a small amount of Cl^- ions is introduced into the electrolyte. Figure 3 shows STM images of Cu growth after the injection of HCl to give a final concentration of 0.3 mM into a solution containing 2 mM $CuSO_4$ and 0.1 M H_2SO_4. One can see that before the Cl^- ions have reached the electrode surface, that is, at $t = 0$ s, the growing Cu steps are very rough over the whole length scale of the images (Figure 3a). However, as soon as the Cl^- adsorption begins, the steps straighten out almost immediately (Figure 3b–d). In addition, the number of steps in the imaged area increases. We suggest that the increase of the number of steps in a Cl^- containing solution is due to a smaller size of the building block, as well as that of the critical nucleus for the formation

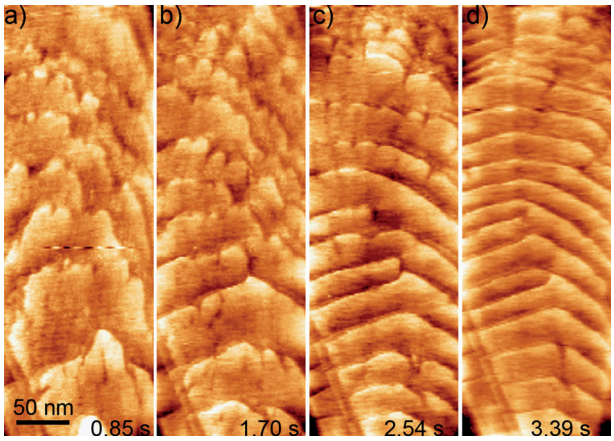

Figure 3. STM images of a growing Cu step bunch at −30 mV vs. Cu/Cu^{2+} after the injection of 0.3 mM HCl into a 2 mM $CuSO_4$ and 0.1 M H_2SO_4 solution (see also the Supporting Information). Adsorption of Cl^- leads to the straightening of the steps as well as to a change of the step orientation. Additionally, the distance between two consecutive steps is significantly reduced after the adsorption of Cl^-.

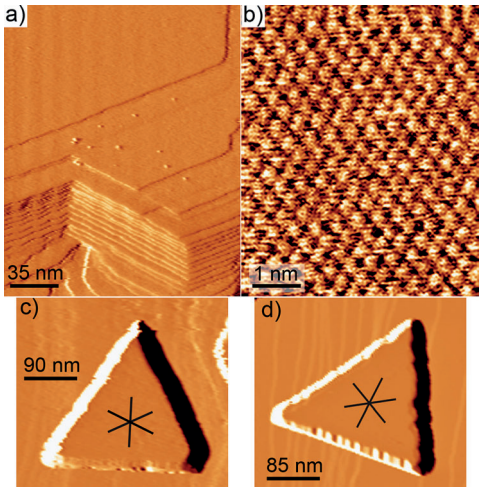

Figure 4. STM images showing the orientation of the Cu steps during Cu deposition. a) Cu steps during deposition. The angle between the steps is 120°. b) Cl^- adlayer on a Cu crystallite imaged after deposition. c) and d) show zoom-out images of the pre-deposited Cu(111) crystallites, on the surface of which (a) and (b) were acquired respectively. The black lines in (c) represent the orientations of the steps in (a) and the black lines in (d) the main symmetry axes of the Cl^- overlayer in (b). The angle between the black lines and the side faces of the Cu crystallites is approximately 30°. Images (a), (c), and (d) are differentiated.

of this building block. As we have mentioned before, the distance between monatomic steps that originate from a screw dislocation is proportional to the radius of the building block [see Equation (1)]. If we compare the distances between the steps in Figure 3a and d, we find that these distances become smaller by approximately three times after the adsorption of Cl^-. If we assume that these steps originate from a single screw dislocation, we may conclude that the radius of the building block in the presence of Cl^- is about 0.47 nm. This value corresponds well to the distance of 0.42 nm between two neighboring Cl atoms of the Cl adlayer on the Cu(111) surface.[12] Additionally we find that the propagation speed of the steps is higher by at least a factor of 3 in Figure 3d as compared to Figure 3a.

Additionally, we observe that the orientation of the propagating monatomic Cu steps changes after the injection of Cl^- into the electrolyte. By comparing the step orientation with the orientation of the side faces of the predeposited Cu(111) crystallites, on which the Cu steps were grown, we find that the growing monatomic steps make an angle of approximately 30° with the main crystallographic directions of the Cu(111) surface (Figure 4a and b). We measure the same angle of approximately 30° between the close-packed directions of the Cl^- adlayer and the main crystallographic directions of the Cu(111) (Figure 4c and d). Thus, we can conclude that the growing Cu steps are not oriented along the close-packed directions of Cu(111), but along the close-packed direction of the Cl^- overlayer. Preferential orientation of the Cu steps on Cu(111) along the close-packed direction of the Cl^- adlayer has been also observed by Wandelt and coworkers.[13] A similar observation has been made for Cu(100) during Cu deposition and dissolution in a Cl^- containing electrolyte.[5] The Cu steps align along the close-packed direction of the c(2×2) Cl overlayer. In addition, deposition occurred in $(\sqrt{2}\times\sqrt{2})R45^\circ$ units, which consist of two Cu atoms and one adsorbed Cl atom.

In agreement with the literature, in our experiments the addition of small amounts of Cl^- into a Cu-sulfate-based plating bath has an accelerating effect on Cu deposition. Indeed, from Figure 3 we could derive that both the step density and the step-propagation speed increase after the injection of Cl^- into the solution, thus leading to an increased Cu deposition rate. A question arises whether the observed acceleration effect can be ascribed solely to the formation of a complex between Cl^- and Cu^+.[6] The formation of the Cu^+-Cl complex should increase the deposition speed by an increase in the supply of the material to the electrode surface. In turn, this increase in the supply of the material should lead to a higher step-propagation speed. But the density of the monatomic steps should not increase, since it is proportional to the size of the building block, and the latter should not depend on the flux of the material to the electrode surface. In addition, the modification of the structure of the anion adlayer and the change of the step orientation, such as that shown in Figure 3, cannot be explained by the formation of Cu^+-Cl complexes. In the following we will discuss the possible structural effect of the anions on the electrodeposition kinetics of Cu.

In general, one can distinguish two steps in the process of the conversion of an ion from the double-layer region into the metallic atom incorporated into the metal lattice.[14] The first step is the conversion of a metal ion, such as Cu^{2+}, into an adatom (or a partially charged ad-ion) that is adsorbed on the electrode surface. The second step is the incorporation of the adatom (ad-ion) into the crystal lattice of the electrode. These two steps can proceed either consecutively, as in the case of deposition with active surface diffusion, or simultaneously, if the deposition occurs through the direct-attachment mecha-

nism. Both these steps can influence the kinetics of electrodeposition. Hence, in the case of Cu deposition, formation of the Cu^{+}-Cl complex could enhance the rate of the transition from Cu^{2+} to Cu adatom state, thereby accelerating the deposition. On the other hand, the lowering of the incorporation barrier into the crystal lattice for an adatom would lead to a higher propagation speed of atomic steps, and also enhance the deposition rate.

We have shown above that, in a SO_4^{2-} containing but Cl^- free electrolyte, growth of a Cu layer on a Cu(111) surface proceeds in complete units of the moiré pattern, each of which contains over 40 Cu atoms (Figure 5a). By analogy, we

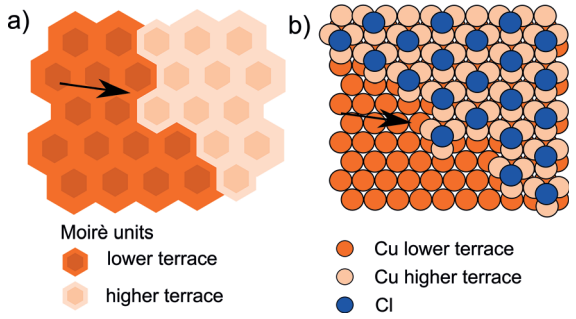

Figure 5. A model of the structure of Cu steps in a sulfate-containing but Cl^- free electrolyte (a) and a Cl^- containing one (b). The arrows point to the stable building blocks of the steps. For simplicity, the building block in (b) is schematically drawn consisting of three Cu atoms and one Cl atom. Please note that in (a) the relative position of the lower and the higher terrace is approximate and in (b) the Cl atoms on the lower terrace are not shown.

expect a similar growth behavior in a Cl^- containing solution with a stable growth unit of a few Cu atoms and some Cl atoms on top. We have estimated above that the radius of the building block in the presence of Cl^- is 0.47 nm, which would correspond to approximately 9 Cu atoms and 3 Cl atoms. However, this still has to be verified experimentally. Such a building block is similar to the building block of two Cu atoms and one Cl atom that is found on Cu(100) in a Cl^- containing solution.[5] It is important that the number of atoms that constitute to this building block is much smaller than in the case in the absence of Cl^- (Figure 5b). The fact that a stable building block consists of more than one Cu atom implies that there is a certain energy barrier (nucleation barrier) associated with the formation of the critical nucleus for this stable block. It is probable that the size of the critical nucleus for a stable, 40 atom building block is significantly larger than that for a stable building block of only a few atoms, thus leading to a lower probability of the formation of a larger block under the same electrodeposition conditions. This finding in turn suggests that in the Cl^- free electrolyte a larger barrier could exist for the incorporation of the Cu^{2+} ions into the metallic crystal of the deposit relative to the incorporation barrier in the Cl^- containing electrolyte. Thus, the accelerating effect of the Cl^- ions on the electrochemical Cu deposition from sulfate-based solutions could partly be due to the lower barrier and hence faster kinetics of the incorporation of the Cu^{2+} ions into the growing deposit.

In summary, we have demonstrated for the first time, on the example of Cu electrodeposition in the presence of Cl^-, that additives can influence the deposition rate by inducing structural changes on the atomic level. We expect our findings to be of a more general nature and therefore realized also on other metals and/or with other additives. Also, similar effects could be expected during crystal growth from supersaturated solutions or deposition from a gas phase.

Experimental Section

All STM measurements were performed with a custom-built fast electrochemical STM equipped with a home-built quartz electrochemical flow cell.[7] Tungsten tips coated with polyethylene were used for imaging. All STM images were acquired in constant current mode at −5 mV tip bias, ca. 500 pA tunneling current, and 1.18 Hz imaging rate. Before each experiment, the Au(111) single-crystal substrate was prepared by immersion into a freshly-prepared piranha solution, rinsing in ultra-pure water, and subsequent annealing at light-yellow heat in a butane flame for approximately 10 min. Immediately after cooling down, the crystal was mounted in the flow cell, and a drop of either the working electrolyte or ultra-pure water was put onto the surface to prevent possible surface contamination from the air. The electrolytes were prepared from suprapure H_2SO_4 and HCl (Merck), 99.999% $CuSO_4$ (Alfa Aesar), and ultrapure water (MilliQ).

Received: September 12, 2012
Revised: December 19, 2012
Published online: January 23, 2013

Keywords: accelerator · additive · copper · crystal growth · electrodeposition

[1] a) A. I. Danilov, E. B. Molodkina, A. V. Rudnev, Y. M. Polukarov, J. M. Feliu, *Electrochim. Acta* **2005**, *50*, 5032; b) L. Guo, S. Zhang, P. C. Searson, *Phys. Rev. E* **2009**, *79*, 051601; c) A. Radisic, J. G. Long, P. M. Hoffmann, P. C. Searson, *J. Electrochem. Soc.* **2001**, *148*, C41; d) M. Willis, R. Alkire, *J. Electrochem. Soc.* **2009**, *156*, D377; e) P. M. Rigano, C. Mayer, T. Chierchie, *Electrochim. Acta* **1990**, *35*, 1189; f) G. Oskam, P. M. Vereecken, P. C. Searson, *J. Electrochem. Soc.* **1999**, *146*, 1436; g) U. Emekli, A. C. West, *J. Electrochem. Soc.* **2010**, *157*, D257; h) M. Zheng, M. Willey, A. C. West, *Electrochem. Solid-State Lett.* **2005**, *8*, C151.

[2] a) R.-Q. Song, H. Cölfen, *CrystEngComm* **2011**, *13*, 1249; b) X. X. Li, X. D. Xu, Y. Y. Dan, M. L. Zhang, *Crystallogr. Rep.* **2008**, *53*, 1261.

[3] M. J. Rost, *Phys. Rev. Lett.* **2007**, *99*, 266101.

[4] a) S. Morin, A. Lachenwitzer, O. M. Magnussen, R. J. Behm, *Phys. Rev. Lett.* **1999**, *83*, 5066; b) A. Lachenwitzer, S. Morin, O. M. Magnussen, R. J. Behm, *Phys. Chem. Chem. Phys.* **2001**, *3*, 3351; c) S. Strbac, F. Maroun, O. M. Magnussen, R. J. Behm, *J. Electroanal. Chem.* **2001**, *500*, 479; d) W. H. Li, J. H. Je, S. F. Y. Li, R. J. Nichols, *Surf. Sci.* **2000**, *449*, 207; e) F. Golks, J. Stettner, Y. Gründer, K. Krug, J. Zegenhagen, O. M. Magnussen, *Phys. Rev. Lett.* **2012**, *108*, 256101.

[5] a) O. M. Magnussen, W. Polewska, L. Zitzler, R. J. Behm, *Faraday Discuss.* **2002**, *121*, 43; b) W. Polewska, R. J. Behm, O. M. Magnussen, *Electrochim. Acta* **2003**, *48*, 2915.

[6] Z. Nagy, J. P. Blaudeau, N. C. Hung, L. A. Curtiss, D. J. Zurawski, *J. Electrochem. Soc.* **1995**, *142*, L87; W. Shao, G. Pattanaik, G. Zangari, *J. Electrochem. Soc.* **2007**, *154*, D201.

[7] Y. I. Yanson, F. Schenkel, M. J. Rost, *Rev. Sci. Instr.* 2013, in print, AIP ID Code 082301RSI.
[8] M. Wilms, P. Broekmann, C. Stuhlmann, K. Wandelt, *Surf. Sci.* **1998**, *416*, 121.
[9] P. Broekmann, M. Wilms, A. Spaenig, K. Wandelt, *Prog. Surf. Sci.* **2001**, *67*, 59.
[10] a) W. K. Burton, N. Cabrera, F. C. Frank, *Philos. Trans. R. Soc. London Ser. A* **1951**, *243*, 299; b) N. Cabrera, M. M. Levine, *Philos. Mag.* **1956**, *1*, 450.
[11] E. Budevski, G. Staikov, V. Bostanov, *J. Cryst. Growth* **1975**, *29*, 316.
[12] Y. Gründer, A. Drünkler, F. Golks, G. Wijts, J. Stettner, J. Zegenhagen, O. M. Magnussen, *Surf. Sci.* **2011**, *605*, 1732.
[13] a) D. W. Suggs, A. J. Bard, *J. Am. Chem. Soc.* **1994**, *116*, 10725; b) P. Broekmann, M. Wilms, M. Kruft, C. Stuhlmann, K. Wandelt, *J. Electroanal. Chem.* **1999**, *467*, 307.
[14] J. O. M. Bockris, A. K. N. Reddy, M. Gamboa-Aldeco, *Modern Electrochemistry 2A: Fundamentals of Electrodics*, Kluwer Academic, Amsterdam, **2000**, pp. 1296 – 1301.

